Dynamics of the superprotonic conductor $K_9H_7(SO_4)_8 \cdot H_2O$ studied by means of nuclear magnetic resonance

2004 J. Phys.: Condens. Matter 16 7967

(http://iopscience.iop.org/0953-8984/16/45/019)

INSTITUTE OF PHYSICS PUBLISHING JOURNAL OF PHYSICS: CONDENSED MATTER

J. Phys.: Condens. Matter **16** (2004) 7967–7977 PII: S0953-8984(04)85493-6

Dynamics of the superprotonic conductor $K_9H_7(SO_4)_8 \cdot H_2O$ studied by means of nuclear magnetic resonance

S Vrtnik[1], T Apih[1], M Klanjšek[1], P Jeglič[1], G Lahajnar[1], L F Kirpichnikova[2], A I Baranov[2] and J Dolinšek[1]

[1] J Stefan Institute, University of Ljubljana, Jamova 39, SI-1000 Ljubljana, Slovenia
[2] Shubnikov Institute of Crystallography, Russian Academy of Sciences, Leninskii Prospekt 59, Moscow, 117333, Russia

Received 27 August 2004, in final form 22 September 2004
Published 29 October 2004
Online at stacks.iop.org/JPhysCM/16/7967
doi:10.1088/0953-8984/16/45/019

Abstract

The dynamics of a recently discovered superprotonic conductor $K_9H_7(SO_4)_8 \cdot H_2O$ has been studied between 40 and 425 K by techniques based on the NMR spectrum shape, spin–lattice and spin–spin relaxation. At low temperatures (such as 40 K), proton intra-H-bond hopping is already intensive. At higher temperatures, water 180° reorientations become observable in the NMR experiments, whereas above 250 K, proton interbond jumps—a precursor of the superprotonic conductivity above the transition temperature $T_{sp} = 398$ K—become frequent. Above T_{sp}, a large increase in the proton spin–spin relaxation time T_2 indicates that proton long-range diffusion becomes significant. Proton interbond jumps are assisted by reorientations of the SO_4 tetrahedra, which also cause breaking of the water bonds, so water molecules become free and consequently diffuse out of the crystal. The loss of water allows rearrangement of the lattice, so the number of structurally equivalent proton sites in the superprotonic phase is increased, resulting in a very open structure for the hydrogen interbond transfer.

1. Introduction

Many hydrogen-bonded insulating crystals become good protonic conductors at elevated temperatures, some exhibiting a superprotonic conducting phase of electrical conductivity up to $\sigma \approx 10^{-2}\ \Omega^{-1}\ \mathrm{cm}^{-1}$ [1]. In a search for new superionic conductors, high protonic conductivity was discovered in a series of hydrate compounds of acid alkali salts [2–10] with the general formula $M_mH_n(AO_4)_p \cdot xH_2O$, where $0 < x \leqslant 1$, M = K, Rb, NH_4, Cs and A = S, Se, P. The best studied examples are $Cs_5H_3(SO_4)_4 \cdot xH_2O$ and $Cs_5H_3(SeO_4)_4 \cdot xH_2O$ crystals [2, 3, 7–10], where acid protons are mainly responsible for the high protonic conductivity, whereas

crystalline water molecules play a special role in the stabilization of the high-temperature superprotonic phase. In a recent study [5, 6] of the influence of the K–Cs substitution on the properties of the superprotonic phase, attempts were made to grow pentapotassium trihydrogen tetrasulfate monohydrate crystals. Surprisingly, the chemical formula of the newly synthesized compound appeared to be $K_9H_7(SO_4)_8{\cdot}H_2O$ (abbreviated as NKHS in the following). Heat capacity and bulk conductivity measurements [6] confirmed that this compound is a superprotonic conductor, undergoing a first-order phase transition to the superprotonic phase at $T_{sp} = 398$ K. However, the transition was found to be quasi-reversible, being reversible upon thermal cycling only for the monohydrate form of the crystal. The microscopic model of the phase transition needs further consideration due to the rich structure of the H-bond network, involving bifurcated hydrogen bonds and apparently also oxonium H_3O^+ ions, while the influence of water content on the protonic conductivity is not well understood as well.

In order to elucidate the dynamics of the superprotonic phase transition in the NKHS, we performed a ^{1}H nuclear magnetic resonance (NMR) study on a virgin monohydrate crystal by employing various NMR techniques that probe hydrogen dynamics on different timescales:

(i) NMR line shape and spin–spin relaxation studies that probe atomic motions in the kHz range and
(ii) spin–lattice relaxation studies that are sensitive to motions in the 100 MHz range.

A combination of these 'multi-clock' experiments should enable us to resolve three major contributions to the hydrogen dynamics in the NKHS both below and above T_{sp}, namely the acid proton intra-H-bond jumps, the inter-H-bond jumps leading to the protonic conductivity and the 180° flips of water molecules, accompanied by water diffusion out of the crystal in a dehydration process upon heating.

2. Structural considerations

The crystal structure of NKHS at room temperature was determined recently by Dilanyan *et al* and the details will be published elsewhere [11]. There remains some ambiguity as regards the position of the hydrogen atom H(7) in the unit cell, so the exact chemical formula of the compound is either $K_9H_6(SO_4)_8H{\cdot}H_2O$ or $K_9H_6(SO_4)_8{\cdot}H_3O$. At room temperature the lattice has a pseudohexagonal symmetry with a monoclinic distortion (space group $P2_1/c$) and lattice parameters $a = 7.076$ Å, $b = 19.825$ Å, $c = 23.505$ Å and $\beta = 95.42°$ with four formula units per unit cell ($Z = 4$). The independent region of the unit cell contains nine K^+ cations and eight $(SO_4)^{2-}$ anions (figure 1), which are characterized by distorted tetrahedral coordination. There are two kinds of hydrogen bonds in the structure, six strong acid bonds with the lengths between 2.54 and 2.72 Å and two water–sulfate O_w–$H_w(1)\cdots O(17)$ and O_w–$H_w(2)\cdots O(16)$ bonds. A specific feature of the H-bond network in NKHS is a bifurcated bond $O(12)$–$H(1)\cdots O(15)\cdots H(2)$–$O(24)$. The above-mentioned hydrogen atom H(7) has two possible sites (figure 1(b)). One is between O(12) and O(23) atoms, where H(7) would form a weak bond of length 2.993 Å. In this case the chemical formula of NKHS should be $K_9H_6(SO_4)_8H{\cdot}H_2O$. The second possibility is to place H(7) between water oxygen O_w and oxygen O(4), where an oxonium ion H_3O^+ is formed and the chemical formula becomes $K_9H_6(SO_4)_8{\cdot}H_3O$. The symmetry of the high-temperature phase has not been determined as yet, but it is presumably hexagonal and the network of acid hydrogen bonds and the molecular layers of crystalline water probably undergo a dynamic disordering at the phase transition point. The thermogravimetric and infrared (IR) spectroscopic data [4] indicate loss of crystalline water in the superprotonic phase. The water is considered to play a crucial role

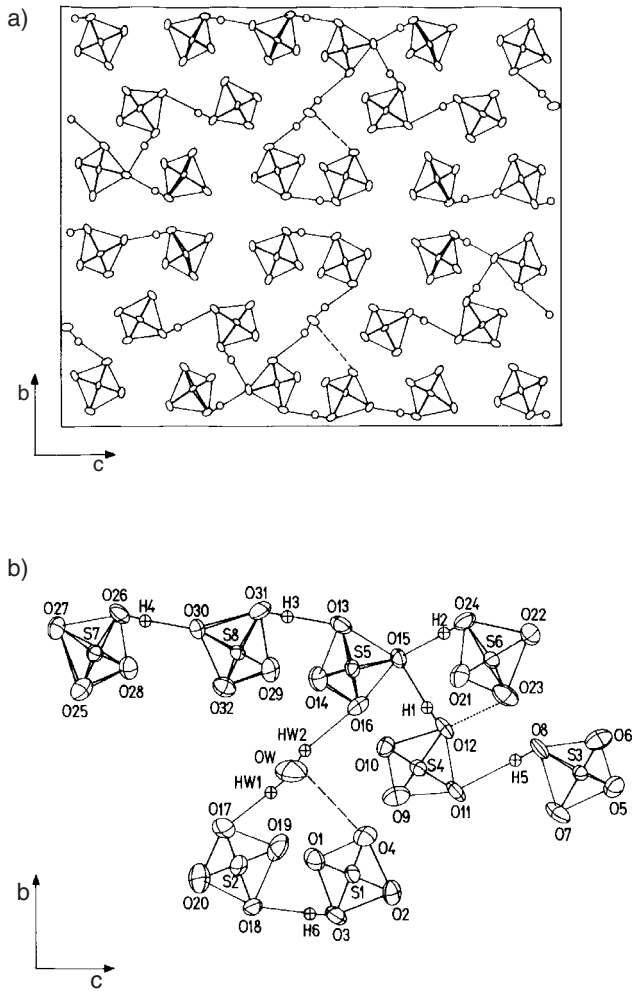

Figure 1. (a) Projection of the $K_9H_7(SO_4)_8{\cdot}H_2O$ room temperature crystal structure (assumed to be $K_9H_6(SO_4)_8{\cdot}H_3O$) onto the (b, c) plane (potassium atoms not shown). (b) The independent region of the unit cell with two possibilities for the hydrogen H(7) position (dashed line: O_w–H(7) $\cdots$ O(4); dotted line: O(12)–H(7) $\cdots$ O(23)).

in the stabilization of the low- and high-temperature phases—the stoichiometric water content ($x = 1$) stabilizes the poorly conducting low-temperature phase, while the loss of water stabilizes the highly conducting superprotonic phase. The loss of water allows rearrangement of the lattice, so the number of structurally equivalent proton sites in the superprotonic phase becomes larger than the number of mobile protons, resulting in a very open structure for the hydrogen interbond transfer. Here it is important to stress that the first-order superprotonic transition can be observed upon heating only in the first thermal cycle performed on a virgin (equilibrium monohydrate structure) crystal [6], whereas in a subsequent cooling run, the superprotonic phase is supercooled down to room temperature. However, this quenched state is metastable, because the inverse process of hydration becomes possible. In the ambient air at room temperature the crystal recovers its original monohydrate structure in the course of days or weeks, and the phase transition occurs as before.

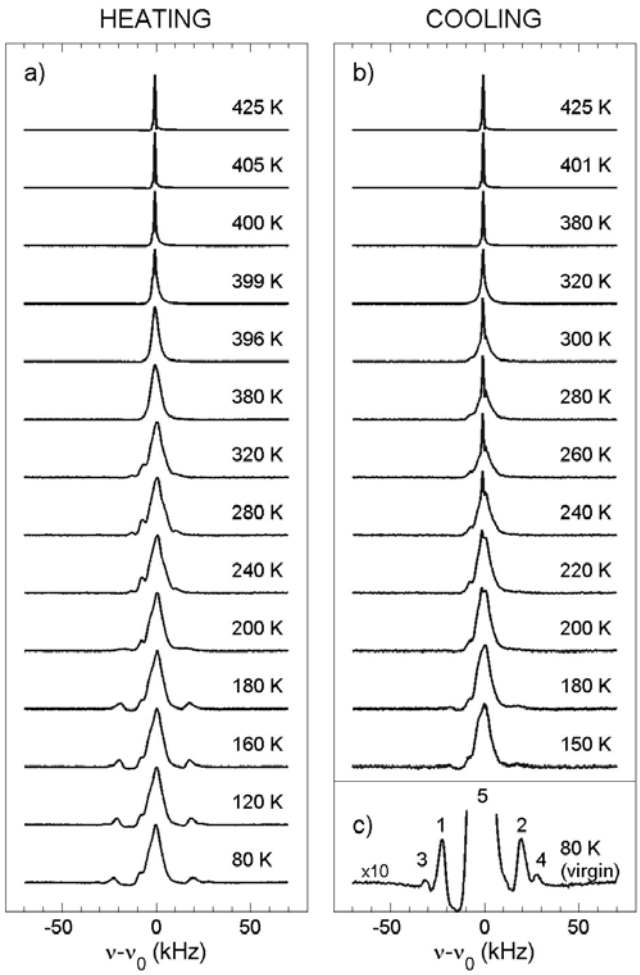

Figure 2. Temperature-dependent proton spectra of a $K_9H_7(SO_4)_8{\cdot}H_2O$ monocrystalline sample ($\nu_0(^1H) = 200$ MHz). (a) The heating run on a virgin sample starting at 80 K and (b) a subsequent cooling run starting from the superprotonic phase. The peak assignment (1–4 for the water lines and 5 for the acid proton line) is shown in (c), where the 80 K spectrum of a virgin sample is replotted on a ten-times-expanded vertical scale.

3. Results

3.1. The proton NMR spectrum

The proton NMR spectrum of a monocrystalline NKHS sample (in a monohydrate form) was measured at the resonance frequency $\nu_0(^1H) = 200$ MHz in the temperature interval between 80 and 425 K. A one-pulse sequence with the rf pulse length of 4 μs was used. The spectrometer dead time of 8 μs caused slight distortion of the line shape as regards the intensity variation over the spectrum. As there are two kinds of protons in the NKHS structure—the acid and the water protons—the rigid lattice NMR spectrum at low temperatures is expected to exhibit a structure. The seven acid and the two water protons should yield two superimposed lines with an intensity ratio 7:2. The acid protons are expected to yield a

featureless spectrum (of approximately Gaussian shape) with a width similar to that found for the related $Cs_5H_3(SO_4)_4{\cdot}H_2O$ compound [8], where the full width at half-height (FWHH) at low temperatures amounted to 10 kHz. As regards the spectrum of the water protons, the orientations of the water molecules are at low temperatures expected to be randomly frozen out, so the water proton spectrum should be a Pake doublet with the separation between maxima of about 10 G (equivalent to 43 kHz in the frequency scale) [12]. The temperature-dependent proton NMR spectra were measured in temperature steps of 10 K (and in smaller steps close to the transition temperature T_{sp}) in one complete heating–cooling cycle starting with the virgin sample at 80 K, going into the superprotonic phase up to 425 K and then cooling back to 150 K. A collection of spectra obtained in a heating run is displayed in figure 2(a). The spectrum of the virgin sample at the lowest temperature investigated, 80 K, may be analysed by assuming it to be a rigid lattice spectrum. The spin–lattice relaxation data, to be presented in the following, demonstrate that this assumption is correct for the water proton spectrum, whereas it is not justified for the acid protons, which already perform frequent intrabond jumps at that temperature. The spectrum at 80 K exhibits a structure of a high-intensity central part and two low-intensity side peaks located at $\nu - \nu_0 = -24$ and +20 kHz (marked as 1 and 2 in figure 2(c), where this spectrum is displayed on a ten-times-magnified vertical scale). In addition, two tiny outer peaks at −31 and +28 kHz (marked as 3 and 4) are also evident, their intensities being much smaller than those of the peaks 1 and 2. The FWHH $\Delta\nu_{1/2} \approx 10$ kHz of the central part (marked as 5 in figure 2(c)) is very similar to that of the acid proton line in the $Cs_5H_3(SO_4)_4{\cdot}H_2O$. Its intensity is also much larger than that of the side peaks, so it is straightforward to assign this line to the acid protons of the NKHS structure. The shape of the central part is not completely featureless, but exhibits unresolved shoulders that indicate the existence of fine structure in the acid proton spectrum of the monocrystalline sample. The two side peaks 1 and 2 are separated by 44 kHz, which is typical splitting for the proton pair of a crystalline water molecule. Though this doublet of peaks appears as two sharp lines (that would indicate an ordered sublattice of crystalline water molecules at low temperature), we cannot rule out the possibility that these peaks are in fact the singularities of the continuous Pake spectrum (due to randomly frozen-out water orientations at low temperature) whose intensity is so low that only the singularities are visible. The nonobservability of the continuous intensity in between the singularities could be an experimental problem caused by the spectrometer dead time that cuts the rapidly decaying free-induction signal of the broad spectral component. Similarly, the two tiny peaks 3 and 4, separated by 59 kHz, may be viewed as singularities of another continuous spectrum of either a proton doublet of two more strongly interacting protons (slightly smaller distance in space) or, more likely, a proton triplet in the case of an H_3O^+ oxonium ion. The NMR spectrum at 80 K is thus a sum of the overlapping spectra of a relatively narrow, high-intensity acid proton spectrum and the broader crystalline water spectrum. The intensities of the acid and the water proton spectra qualitatively agree with the theoretical ratio 7:2, but a quantitative comparison is hampered by the overlap of the two spectra and the dead-time distortion of the line shape. The temperature dependence of the peaks in the spectrum in a heating run is displayed in figure 3. Upon heating from 80 K, the splitting of the peaks 1–4 (referred to as the water peaks) gradually decreases until at 200 K the peaks can no longer be traced (they become hidden behind the high-intensity acid proton line), so the crystalline water spectrum is obviously destroyed by molecular motion. Such a line shape transition of the water spectrum may be attributed to 180° flips of the water molecules, which in the temperature range from 80 to 200 K speed up from frequencies smaller than the Pake-doublet width (of several tens of kilohertz) to higher frequencies. In this thermally activated motion, the traceless proton dipole–dipole interaction is averaged to zero by fast reorientation of the water molecules, producing motional narrowing of the water spectrum. As the water

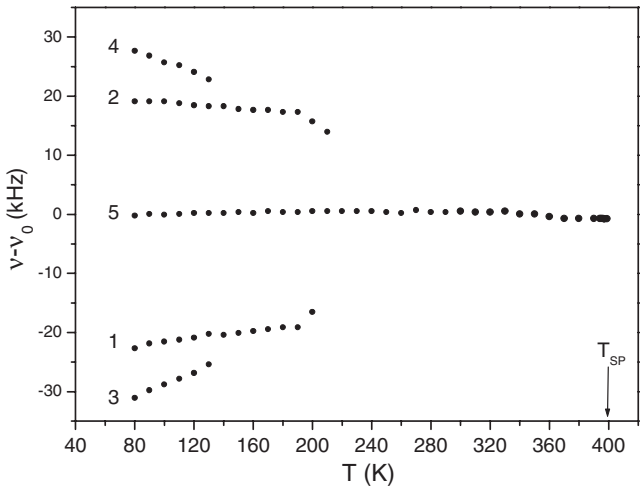

Figure 3. The temperature dependence of the peaks in the proton spectrum of NKHS in a heating run. The peaks 1–4 are due to water protons, whereas peak 5 is due to acid protons (see figure 2(c)).

peaks cannot be traced at temperatures higher than 200 K, a quantitative extraction of the activation energy and the correlation time from the line shape motional transition could not be made. Regarding the temperature dependence of the acid proton line in the same temperature interval (80–200 K), there is not much change in the line shape. As the small-scale proton intra-H-bond jumps are not similar to isotropic-like Brownian motion, they are also not expected to produce a substantial narrowing of the acid proton line. The analysis of the ^{1}H spin–lattice relaxation time T_1, to be presented in the next section, shows that the intrabond motion of the acid protons is considerably faster than the water proton dynamics in the same temperature interval.

Upon further heating above 200 K, the acid proton line starts to narrow as well (figure 2(a)). In the close vicinity of the superprotonic phase transition at $T_{sp} = 398$ K, the spectrum undergoes a complete motional narrowing, consisting of a single narrow line at the Larmor frequency. The motion of the protons in the superprotonic phase is thus liquid-like, so the dipolar interaction between protons is averaged out to zero. The residual linewidth of FWHH 1 kHz may be attributed to the inhomogeneity of the external magnetic field.

An interesting hysteresis effect of supercooling the high-temperature superprotonic phase is observed when subsequently cooling the sample from the highest temperature 425 K reached in the superprotonic phase. A set of spectra in the cooling run is displayed in figure 2(b). The spectrum retains its motionally averaged shape down to almost room temperature, whereas at lower temperatures, a motional transition sets in. A broad component in the spectrum appears that coexists with the motionally narrowed line in the temperature interval between about 300 and 200 K. Below 200 K, the narrow component has disappeared completely, whereas the shape and width of the broad spectrum closely resemble those of the acid protons of the virgin sample. There is no trace of the water peaks down to the lowest investigation temperature of 150 K, so the crystalline water has obviously left the crystal, in agreement with the thermogravimetric and IR data [4]. This fact gives unambiguous confirmation that the peaks 1–4 are due to the water protons of the NKHS structure. Therefore, the proton spectrum in a cooling run demonstrates that the superprotonic phase is supercooled down to room temperature and that some fast-moving protons are present even down to 200 K (where the motionally narrowed

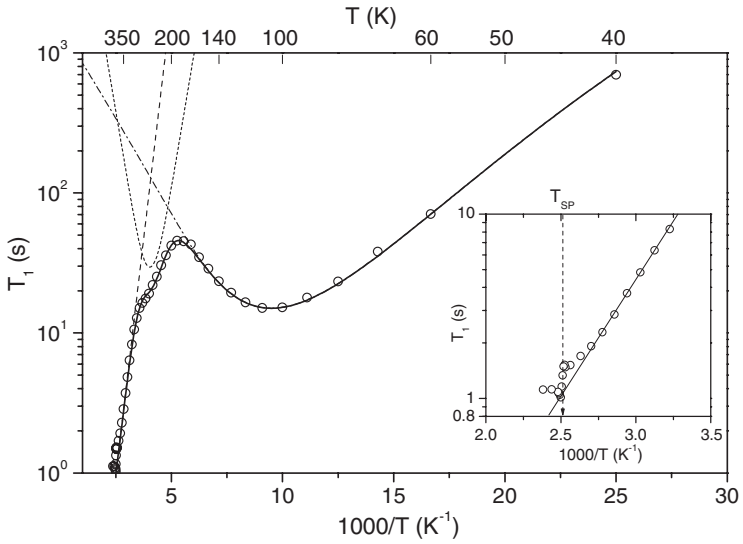

Figure 4. The proton spin–lattice relaxation time T_1 of NKHS in a $\ln T_1$ versus $1000/T$ plot between 40 and 420 K. The solid curve is the theoretical fit using equation (4) with the fit parameters given in the text. The three relaxation contributions to $1/T_1$ are shown separately (dashed–dotted line—proton intrabond jumps; short-dashed line—water reorientations; long-dashed line—proton interbond jumps). The inset shows T_1 on an expanded temperature scale in the vicinity of the superprotonic transition at $T_{sp} = 398$ K.

line disappears completely), which is as much as $\Delta T \approx 200$ K below T_{sp}. The fact that no water peaks were observed any longer at low temperature after the sample was heated to the superprotonic phase supports the hypothesis on the role of water in the NKHS crystal—the water stabilizes the low-temperature nonconducting phase whereas the loss of water stabilizes the superprotonic phase.

The existence of two kinds of water peaks in the virgin (monohydrate) sample deserves special comment. While the separation of the higher-intensity peaks 1 and 2 of 44 kHz at 80 K is typical for the proton pair of a crystalline water molecule, the separation of the low-intensity pair 3, 4 of 59 kHz is considerably larger. A straightforward—but yet to be proven—assignment of the 3, 4 pair can be made on the basis of the NKHS structure. As discussed above, the position of the hydrogen atom H(7) is not clear—it can either be located between the O(12) and O(23) atoms, or it can be located between the water oxygen O_w and the oxygen O(4), forming an oxonium H_3O^+ ion. In the case of an H_3O^+ ion, the protons are arranged in a triplet so they interact more strongly and the splitting of the singularities in the spectrum (which should in this case number three [13]) is larger. Our ^{1}H NMR spectrum results are, therefore, compatible with the presence of a small fraction of oxonium ions (due to low intensity of the corresponding NMR signal) that coexist with the abundant 'normal' water. It is possible that the NKHS structure exhibits domains with both kinds of H(7) bondings to the nearby SO_4 tetrahedra. Due to the small intensity of the water NMR signals, a quantitative evaluation of the two fractions is uncertain.

3.2. Proton spin–lattice relaxation

The proton spin–lattice relaxation time T_1 was measured using the inversion–recovery technique and the T_1 data are displayed in figure 4 in a $\ln T_1$ versus $1000/T$ plot. In order

to perform the measurements on a virgin sample, another sample was taken from the same batch as the one used for the line shape measurements. In the temperature range investigated between 40 and 420 K, T_1 exhibits variety of features. At the lowest investigation temperature, 40 K, T_1 is rather long, amounting to 700 s. On going to higher temperatures, T_1 first decreases to the minimum at 110 K, exhibits a maximum at 190 K and then decreases towards T_{sp} with a significant change of slope at 250 K. At T_{sp}, T_1 exhibits a small discontinuous jump (see the inset in figure 4) and then stays short ($T_1 \approx 1$ s) in the superprotonic phase. The significant shortening of T_1 from 40 K to T_{sp} by a factor of 700 demonstrates the strong temperature-dependent acceleration of the proton dynamics in the NKHS on going toward the superprotonic phase.

The above temperature-dependent T_1 behaviour could be reproduced theoretically (solid line in figure 4) by the following model of proton dynamics. In the low-temperature regime between 40 and 190 K, T_1 is determined by the proton intrabond motion that speeds up upon heating and produces a BPP-like minimum at 110 K, where the proton intrabond jump frequencies cross the nuclear Larmor frequency. The intrabond contribution to T_1 can be written as

$$\left(\frac{1}{T_1}\right)_{\text{in}} = A \int g(E_a^{\text{in}}) \left[\frac{\tau_{\text{in}}}{1+\omega_0^2\tau_{\text{in}}^2} + \frac{4\tau_{\text{in}}}{1+4\omega_0^2\tau_{\text{in}}^2}\right] \mathrm{d}E_a^{\text{in}}. \tag{1}$$

Here the intrabond correlation time is given by the Arrhenius form, $\tau_{\text{in}} = \tau_{\text{in}}^0 \exp(E_a^{\text{in}}/k_B T)$, E_a^{in} is the proton intrabond activation energy, $\omega_0 = 2\pi\nu_0$ and A is the acid–proton dipolar coupling constant. As there are seven acid bonds of different lengths in the NKHS structure, the activation energy E_a^{in} cannot assume a single sharp value, but is instead distributed. For numerical convenience we assumed a Gaussian distribution, $g(E_a^{\text{in}}) = (\sqrt{2\pi\sigma^2})^{-1} \exp[-(E_a^{\text{in}} - \bar{E}_a^{\text{in}})^2/2\sigma^2]$, with the mean activation energy $\bar{E}_a^{\text{in}}$ and the standard deviation σ. In the second temperature regime between the T_1 maximum at 190 K and the temperature 250 K, where the change of slope in T_1 is detected, the variation of T_1 is considerably stronger (its slope is steeper), so the associated motional process is of higher activation energy. An inspection of the NMR spectra in figure 2(a) reveals that, in this temperature range, the spectrum of water protons is already motionally averaged due to fast water 180° reorientations (the water lines disappear at 200 K), so water flipping frequencies are higher than the rigid spectrum width (of several tens of kilohertz). Upon heating above 200 K, the flipping frequencies accelerate into the megahertz range and start to affect the spin–lattice relaxation. The T_1 data in this temperature range exhibit a tendency to produce another minimum close to 250 K, but the minimum is not well resolved as another strong relaxation mechanism sets in (which produces the change of slope at 250 K). The water flipping relaxation rate can be written as

$$\left(\frac{1}{T_1}\right)_{\text{w}} = B\left(\frac{\tau_{\text{w}}}{1+\omega_0^2\tau_{\text{w}}^2} + \frac{4\tau_{\text{w}}}{1+4\omega_0^2\tau_{\text{w}}^2}\right). \tag{2}$$

Here $\tau_{\text{w}} = \tau_{\text{w}}^0 \exp(E_a^{\text{w}}/k_B T)$ is the correlation time for the 180° water flips, E_a^{w} is the corresponding activation energy and B is the water dipolar coupling constant. In the third temperature regime between 250 K and the superprotonic transition T_{sp}, the T_1 decrease is the strongest (the slope is the largest), so there is obviously a third motional mechanism involved, which has the largest activation energy. As there is no trace of another BPP-like T_1 minimum at the highest temperatures investigated, all we can be certain of is that the frequencies of this third motion are on the low-frequency side of the nuclear Larmor frequency. For that reason we use the slow-motion limit ($\omega_0\tau \gg 1$) expression of the relaxation rate given by equation (2)

and write the corresponding relaxation contribution in the compact form

$$\left(\frac{1}{T_1}\right)_3 = C\exp(-E_a^{(3)}/k_BT). \tag{3}$$

Due to the lack of a T_1 minimum, we cannot extract the corresponding correlation time $\tau^{(3)}$ from the experimental data, but only the activation energy $E_a^{(3)}$. This third relaxation mechanism should originate from another kind of proton motion, which becomes excited on approaching the superprotonic phase transition and may be viewed as a precursor of the superprotonic mobility. Very probable motional processes are thermally induced reorientations of the SO_4 tetrahedra, combined with the transfer of the acid protons from one to another hydrogen bond, i.e. the proton interbond transfer as a mechanism of the superprotonic conductivity. As the temperature-dependent T_1 data allow determining the activation energies of all three motional mechanisms involved (E_a^{in}, E_a^{w} and $E_a^{(3)}$), this issue can be further elaborated.

The fit of the experimental data was made with the sum

$$\frac{1}{T_1} = \left(\frac{1}{T_1}\right)_{in} + \left(\frac{1}{T_1}\right)_{w} + \left(\frac{1}{T_1}\right)_3, \tag{4}$$

where the corresponding terms are given by equations (1)–(3). The theoretical curve (solid curve in figure 4) reproduces excellently the experimental data in the whole temperature range from 40 K up to T_{sp}. The model can, however, not reproduce the small discontinuous jump at the first-order transition at T_{sp} (see the inset in figure 4) and the tendency towards a temperature-independent T_1 in the superprotonic phase. The temperature independence of T_1 for $T > T_{sp}$ indicates that the spectrum of motional frequencies in the superprotonic phase becomes 'white', i.e. many different motional degrees of freedom of the proton system and the lattice are excited. Upon calculating the theoretical T_1 curve of figure 4, the following fit parameter values were used. The proton intrabond jump parameters were $\bar{E}_a^{in} = 50.0 \pm 3$ meV, $\sigma = 10.4$ meV, $\tau_{in}^0 = 1.6 \times 10^{-12}$ s and $A = 8.2 \times 10^7$ s^{-2}, the water flipping parameters were $E_a^{w} = 188 \pm 5$ meV, $\tau_w^0 = 0.75 \times 10^{-13}$ s and $B = 3.0 \times 10^7$ s^{-2} whereas the parameters of the third relaxation mechanism were $E_a^{(3)} = 267 \pm 10$ meV and $C = 2400$ s^{-1}. The three relaxation contributions to $1/T_1$ are shown separately in figure 4 (dashed–dotted line—proton intrabond jumps; short-dashed line—water reorientations; long-dashed line—third relaxation mechanism). The value $\bar{E}_a^{in} = 50$ meV is typical for the proton intrabond motion in H-bonded insulators [14], whereas the value $E_a^{w} = 188$ meV is also typical for the 180° water flips. Regarding $E_a^{(3)} = 267$ meV, this value fits well into the range $E_a = 0.23$–0.3 eV of activation energies for the protonic interbond motion found by electrical conductivity measurements [1] in many other acid alkali salts with the general formula $M_mH_n(AO_4)_p$, which also exhibit a superprotonic conducting phase. This matching gives strong support to the hypothesis that the $E_a^{(3)}$-processes are SO_4-assisted proton interbond jumps that start to be thermally excited already far below T_{sp} (note that the $E_a^{(3)}$-relaxation contribution to T_1 is already becoming dominant above 250 K, which is as much as $\Delta T \approx 150$ K below the superprotonic transition). Therefore, the transition to the superprotonic phase in NKHS—though nominally of first order—should be considered close to second order.

3.3. Spin–spin relaxation

The proton spin–spin relaxation time T_2 was measured using the Hahn-echo technique and the data in the temperature interval between 370 and 430 K (i.e. in the vicinity of T_{sp} and in the superprotonic phase) are displayed in figure 5. On crossing T_{sp}, a strong increase of T_2 from a 'solid-like' value 120 μs to a 'liquid-like' value 2 ms is observed. This demonstrates

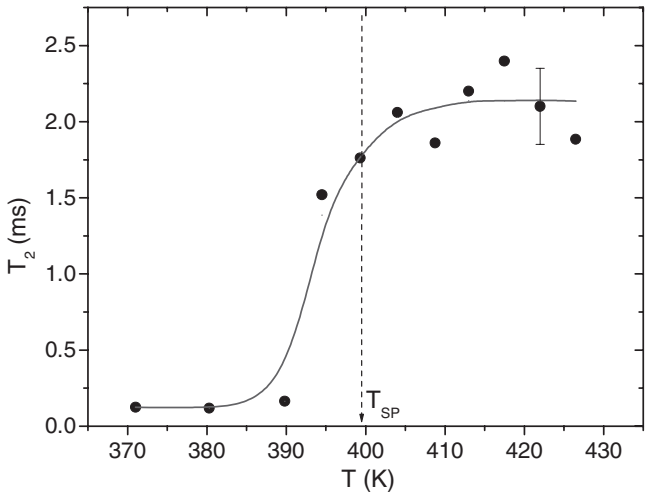

Figure 5. The proton spin–spin relaxation time T_2 of NKHS in the vicinity of T_{sp} and in the superprotonic phase.

the presence of translational diffusion in addition to molecular rotations in the superprotonic phase and is compatible with the high mobility of protons above T_{sp}. It is interesting that T_2 has already started to increase a few degrees below T_{sp}, as a precursor of the phase transition.

4. Discussion

The above results on the temperature-dependent proton NMR spectra and spin–lattice- and spin–spin relaxation times suggest the following picture of hydrogen dynamics in the protonic conductor NKHS. At the lowest temperature investigated (40 K), acid protons already perform frequent intrabond jumps within the O–H $\cdots$ O double-well potentials. The fact that the proton intrabond motion can be described as classical thermally activated over-barrier hopping instead of quantum tunnelling indicates that the jumps are lattice assisted. Due to the existence of seven H bonds of different lengths in the NKHS structure, the intrabond activation energies are distributed around the mean value $\bar{E}_a^{in} = 50$ meV with the standard deviation $\sigma \approx 10$ meV. Upon heating, the intrabond motion speeds up and produces a BPP-like minimum in the spin–lattice relaxation time T_1 at the temperature 110 K, where the proton intrabond jump frequencies cross the nuclear Larmor frequency of 200 MHz. The dynamics of water molecules (considered to be thermally activated 180° reorientation flips with an activation energy $E_a^w \approx 190$ meV) is slower. A motional destruction of the water spectrum is observed around 200 K, where the water flipping frequencies cross the rigid lattice spectrum width of 44 kHz. Upon further heating, the water flipping accelerates into the megahertz range and produces another T_1 minimum at about 250 K, where the flipping frequencies cross the Larmor frequency. At still higher temperatures, between 250 K and the superprotonic transition at 398 K, proton interbond jumps with the activation energy $E_a^{(3)} = 267$ meV—a precursor of the superprotonic conductivity—become the dominant spin–lattice relaxation mechanism. On going to the superprotonic phase, crystalline water diffuses out of the crystal. Due to there being more space in the lattice, SO_4 tetrahedra rotate rather freely, assisting the protons to perform frequent interbond jumps, and the number of unoccupied hydrogen sites is also significantly increased. This results in high superprotonic mobility in the very open hydrogen sublattice.

5. Conclusions

The $K_9H_7(SO_4)_8{\cdot}xH_2O$ crystal is a new superprotonic conductor with a complex structure of the H-bond network. The transition to the superprotonic phase occurs only for the monohydrate ($x = 1$) form of the crystal. The stoichiometric water content stabilizes the poorly conducting low-temperature phase, while the loss of water stabilizes the highly conducting superprotonic phase. The NKHS crystal exhibits a rich hydrogen dynamics. At low temperatures (such as 40 K) proton intrabond hopping is already intense. At higher temperatures, water 180° reorientations become observable in the NMR experiments, whereas above 250 K, proton interbond jumps—a precursor of the superprotonic mobility—become frequent. Above T_{sp}, a large increase in the proton spin–spin relaxation time T_2 indicates that proton long-range diffusion becomes significant. Despite the claimed first-order nature of the superprotonic transition at 398 K, the transition to the superprotonic state may be viewed as a gradual process, where the proton interbond jumps are observed already deeply in the low-temperature phase and their frequency increases on approaching T_{sp}. The mechanism of fast protonic conduction involves both the intra-H-bond proton transfer, O–H $\cdots$ O $\leftrightarrow$ O $\cdots$ H–O, as well as HSO_4 and H_2SO_4 rotation, connected with breaking of the weak part of the O–H $\cdots$ O bond and the formation of a new H bond in a different direction leading to a second HSO_4 or H_2SO_4 ion etc. Fast rotation of the SO_4 tetrahedra also results in breaking of the water bonding, so water molecules become free and consequently diffuse out of the crystal. The loss of water allows rearrangement of the lattice accompanied by a symmetry change at T_{sp}, so the number of structurally equivalent proton sites in the superprotonic phase is increased. This results in very open structure for the hydrogen interbond transfer, which is the microscopic mechanism of the superprotonic conductivity.

References

[1] See, for a review Baranov A I 2003 *Kristallografiya* **48** 1081
Baranov A I 2003 *Crystallogr. Rep.* **48** 1012 (Engl. Transl.)
[2] Baranov A I, Kabanov O A, Merinov B V, Shuvalov L A and Dolbinina V V 1992 *Ferroelectrics* **127** 257
[3] Baranov A I, Kabanov O A and Shuvalov L A 1993 *JETP Lett.* **58** 548
[4] Baranov A I, Sinitsyn V V, Vinnichenko V Yu, Jones D J and Bonnet B 1997 *Solid State Ion.* **97** 153
[5] Baranov A I, Yakushkin E D, Jones D J and Roziere J 1999 *Solid State Ion.* **125** 99
[6] Yakushkin E D and Baranov A I 2000 *Fiz. Tverd. Tela* **42** 1474
Yakushkin E D and Baranov A I 2000 *Phys. Solid State* **42** 1517 (Engl. Transl.)
[7] Belushkin A V, Carlile C J and Shuvalov L A 1995 *Ferroelectrics* **167** 21
[8] Fajdiga-Bulat A M, Lahajnar G, Dolinšek J, Slak J, Ložar B, Zalar B, Shuvalov L A and Blinc R 1995 *Solid State Ion.* **77** 101
[9] Yuzyuk Yu I, Dmitriev V P, Loshkarev V V, Rabkin L M and Shuvalov L A 1995 *Ferroelectrics* **167** 53
[10] Lushnikov S G, Belushkin A V, Beskrovnyi A I, Fedoseev A I, Gvasaliya S N, Shuvalov L A and Schmidt V H 1999 *Solid State Ion.* **125** 119
[11] Dilanyan R A, Zorina L V, Narymbetov B J, Baranov A I, Roziere J and Jones D J 2004 at press
[12] Abragam A 1961 *The Principles of Nuclear Magnetism* (Oxford: Clarendon) p 220
[13] Abragam A 1961 *The Principles of Nuclear Magnetism* (Oxford: Clarendon) p 223
[14] Dolinšek J, Arčon D, Zalar B, Pirc R and Blinc R 1996 *Phys. Rev.* B **54** R6811